

# Counter-Rotating Wind Turbine Experimental with Variation of Axial Distance Using Arduino

Muhamad Jafri<sup>1</sup>, Nurhayati<sup>1</sup>, Verdy A Koehuan<sup>1</sup>

<sup>1</sup>Department of Mechanical Engineering, Nusa Cendana University, Kupang, NTT, Indonesia-85000

**Abstract**— Counter-rotating dual-rotor wind turbines that have two rotors rotating in opposite directions on the same axis can operate at high and low speeds. The aerodynamic performance of this type of wind turbine is influenced by several factors including the geometry of the blade, the use of the number of blades, and the axial distance of the rotor. In this study, a variation of the axial distance of the rotor,  $Z/D$ , where  $Z$  is the axial distance of the two rotors and  $D$  is the diameter of the front rotor, namely  $Z/D=0.4, 0.5$ , and  $0.6$  with the same diameter of the two rotors. This study aims to obtain the performance of a counter-rotating wind turbine by maximizing the output power of free airflow. The method used is an experimental method, where the turbine model is made on a laboratory scale and tested using Arduino. The results of the research indicated by the relationship between the variation of the rotor distance to the total power coefficient of the front rotor and the rear rotor, it was found that the highest total power coefficient occurred at a distance of  $Z/D=0.5$ , with the highest value occurring at  $Z/D=0.5$  with a wider TSR range.

**Keywords**— Counter-rotating; aerodynamic performance; wind turbine; rotor distance; Arduino.

## I. INTRODUCTION

Electricity services for people in Indonesia are fully implemented by the Perusahaan Listrik Negara (PLN), whose network has spread widely throughout the region. However, until now, there are still some areas that have not been reached by the PLN electricity network, especially in remote areas that are very far from the PLN electricity network. Therefore, that to connect these areas with high voltage conduction is not economical. Therefore, it is necessary to make efforts to use natural resources around it such as wind, solar, and water energy as a source of cheap electrical energy. To increase available electrical energy for the community and expect the decreasing supply of fossil fuels and cut the negative impact of burning petroleum (fossil) fuels, because the oil and fossil fuel production in Indonesia has decreased by 10% annually while the level of fuel consumption oil increased on average 6% per year. The problem that occurs in Indonesia today is that producing petroleum fuel cannot keep up with the large consumption of fuel oil, so Indonesia imports oil to meet the energy needs of fuel oil every day. This is because there are no production developments at oil refineries and no new oil wells are found. As a solution to the problem, it is necessary to find alternative energy sources for generating electric power.

The wind turbine power generation system can consist of several turbines installed on a wind farm to serve the electricity grid to consumers or coupled with other sources of electrical power generation, [1]. A large-scale electric power generation system utilizing wind energy that has been installed

today in various parts of the world is a power generation system using a horizontal shaft propeller type wind turbine with three blades, [2][3]. The wind turbine rotor is the main key in the process of converting wind kinetic energy into mechanical energy, so an aerodynamic blade geometry design with the best efficiency is necessary to maximize the energy converted. In this case, the phenomenon of airflow around the rotor is very important to be investigated so that the flow wave losses resulting in reduced aerodynamic efficiency can be minimized, [4]. In recent years, several researchers have presented interesting discoveries about a smart model of a three-blade propeller-type wind turbine, known as a counter-rotating wind turbine (CRWT), which can increase the power coefficient of wind turbines higher than the one rotor condition. Investigation of counter-rotating wind turbines performance with the advice tip speed ratio (TSR) to diameter ratio and distance ratio has been successfully carried out through computation fluid dynamic or CFD simulations, [5][6]. The best CRWT performance is obtained at a diameter ratio of  $D_1/D_2=1.0$  with the maximum power coefficient ( $C_{Pmax}$ ) of 0.5219 or an increase in  $\Delta C_{Pmax}=16.49\%$ , higher than a single rotor. Whereas based on the relative TSR the increase is higher than the normalized total power coefficient is 2.2067 for  $D_1/D_2=0.5$  higher than the single rotor.

Many experimental studies at a laboratory-scale have been carried out by Tian et al. [7], Yuan et al. [8], Ozbay et al. [9][10], Wang et al. [11], and Ozbay et al. [12]. Those studies are still being carried out partially on the ratio of the diameter and axial distance ratio of a particular rotor from the CRWT. Research-based on the distance ratio,  $Z/D_1$  ( $Z$  is the axial distance of the two rotors) with a  $Z/D_1$  range of less than 0.1 for  $D_1/D_2$  greater than one, and  $Z/D_1$  greater than or equal to 0.1 for  $D_1/D_2$  less than or equal to one. Each of these studies does not represent CRWT performance over a wider tip speed ratio range.

The use of a mini generator as a power plant coupled with a turbine rotor on a laboratory scale to the CRWT rotor performance is still an important issue in the study of wind turbine rotor aerodynamics performance. Apart from the problem of measurement error, the effect of the low Reynold number on laboratory scale testing also needs to be studied in detail. This study aims to conduct an experimental study of the aerodynamic performance of the counter-rotating wind turbine (CRWT) rotor through laboratory-scale testing. In this study, the axial distance of the rotor,  $Z/D_1$ , in which  $Z$  is the axial distance of the two rotors and  $D_1$  is the diameter of the front rotor, namely  $Z/D=0.4, 0.5$ , and  $0.6$  with the same diameter of both rotors which is 0.944 m at full-scale. Experiments were

carried out to measure the CRWT performance on a laboratory scale through a scale down with the scale coefficient ( $SC=0.3$ ).

## II. EXPERIMENTAL SETUP

The research starts with the process of preparing and manufacturing and installing the main components of the research, namely: test objects, wind tunnels, and test sections, measuring instruments including calibration, sensor and control systems, turbine rotors, turbine housings, towers, and transmission systems. Both single rotor and dual rotor turbine experiments were taken out through testing in the wind tunnel. The wind tunnel used (Fig. 1.) has a test section with a width of 1840 mm ( $6.5D$ ) and a height of 450 mm ( $1.6D$ ) and the highest wind speed of 12 m/s driven by nine fans.

Test scheme of a counter-rotating dual rotor wind turbine with a generator in Fig. 2. Table 1 shows the functions and specifications of measuring instruments and sensors used in research. Block diagram of functional testing of components in microcontroller and sensor systems as well as measuring instrument calibration in Fig. 3. The INA-219 sensor calibration is carried out to determine the ratio of the voltage and current read by the sensor and standard measuring instruments for input voltage from a power supply source. Measurement of voltage and current on the sensor is carried out 11 times at different input voltages, namely from a voltage of 2.5V to 5V. The number of data taken is 200 samples per measurement point every minute, then analyzed using simple statistical methods by calculating the standard deviation and the standard error deviation.

The sampling method uses the Arduino UNO microcontroller and the data logger system is connected to a computer unit so that the test result data are directly displayed on the computer screen in the form of tables and graphs. While the process of converting analog data into digital data is through the INA219 sensor module to measure current and voltage, the photoelectric speed sensor module is applied to measure the rotation rotor connected to the Arduino (Fig. 2). The logger is separate from the Arduino UNO microcontroller. Several led lamps connected to Arduino from 1.2 volts to 4 volts as the load of the CRWT model with mini generator (Fig. 4b).

The blade model used in this study is the full-scale horizontal axis wind turbine adopted from the blade model developed by NORCOWE (Norwegian Centre for Offshore Wind Energy) and the Department of Energy and Process Engineering, Norwegian University of Science and Technology NTNU, Trondheim, Norway [13][14]. The turbine rotor blade was developed through a series of blind tests, followed by several researchers using the airfoil S826 series issued by NREL (National Renewable Energy Laboratory). The CRWT model shown in Fig. 4a is a laboratory-scale turbine model whose performance will be tested with a rotor diameter of 283 mm, diameter ratio  $D_1/D_2=1.0$ , and the rotor distance ratio,  $Z/D_1$  and tower height of  $0.8D$ . Chord length and twist angle profile along span for the blade geometry in Fig. 5 from the experimental results (blind test 4) BT4

reported by Bartl and Sætran (2016) for the rotor turbine with a diameter of 0.944 m in full-scale test [14].

The blade is made through a 3D printing process with a resolution of 0.025 mm using PLA (Polylactic Acid) material. The blade model is made on a laboratory scale with a coefficient ( $SC=0.3$ ) according to the dimensional equivalence of the numerical model. Meanwhile, the test layout is shown in Fig. 2 through the data acquisition system, namely wind speed, rotor rotation, and load.

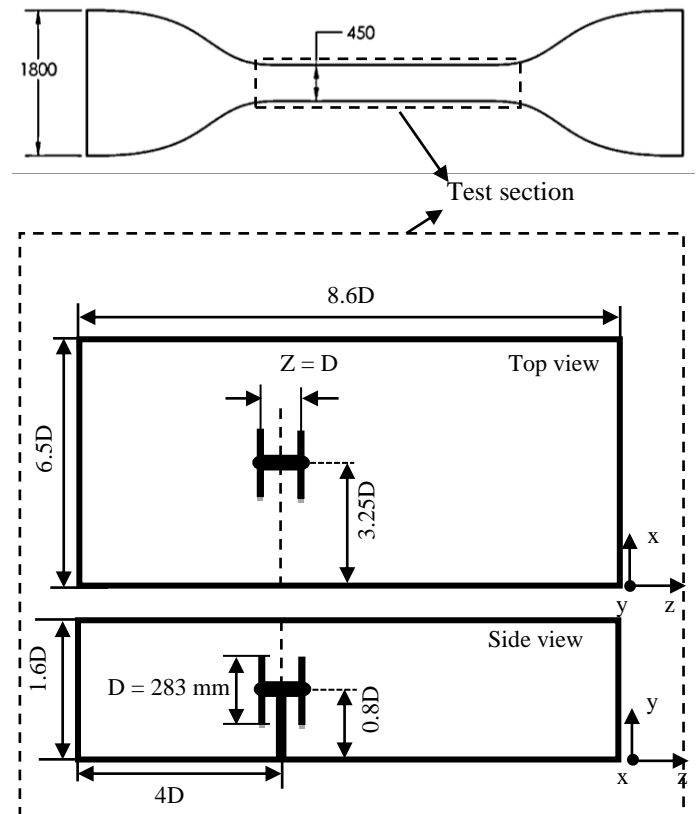


Fig. 1. Wind Tunnel scheme.

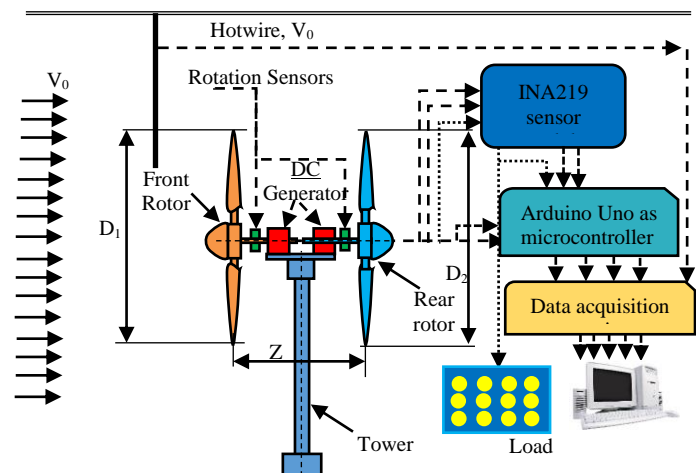


Fig. 2. Test scheme of a counter-rotating dual rotor wind turbine with the generator.

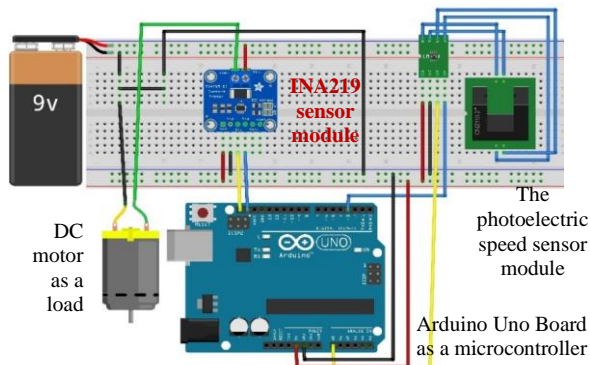


Fig. 3. Block diagram of functional testing of components in microcontroller and sensor systems as well as a measuring instrument calibration.

TABLE 1. Functions and specifications of measuring instruments and sensors used in research.

Device name	range	Resolution	Accuracy	Function
1. Hotwire anemometer	0,1–25 m/s	0,01 m/s	±5%, ±0,1 m/s	Measure wind speed
2. Digital tachometer	2 - 99,999 rpm	0,1 rpm	±0,05% + 1 digit	Measuring rotor rotation (reference)
3. Photoelectric sensors	3-80 cm			Measure rotor rotation
4. INA-219 sensor module	~3.2A and ~+26VDC		±1%	Measure current and voltage

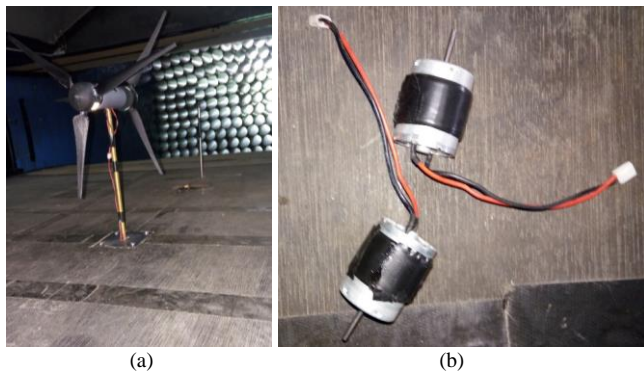


Fig. 4. (a) CRWT model and (b) DC mini generator, voltage rated: 0.01 Volt to 20 Volt, Speed rated: 200-6000 rpm

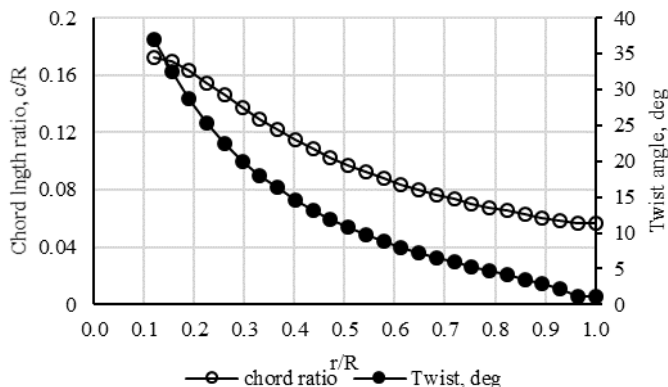


Fig. 5. Chord length and twist angle profile for blade geometry developed by NTNU using airfoil S826 series from NREL [14].

Data collection was carried out by direct observation of the readings of measuring instruments from each sensor used with 200 data samples per measurement point per minute, which were then digitally processed to the data acquisition unit and the computer. Wind speed data are generated by hotwires installed at several points for horizontal and axial positions in front of the rotor. The data generated by the readings of measuring instruments were analyzed using simple statistical methods by calculating the standard deviation and standard error deviation from the average measured value of each sample. Standard deviation is used to evaluate the level of spread of measuring data against the measuring average, while standard deviation is used to assess the level of accuracy of the measured average value against the average value of the standard measuring instrument.

Data analysis was performed to obtain the power coefficient of the counter-rotating horizontal axis wind turbine. The turbine power coefficient ( $C_p$ ) is the ratio between the output power ( $P_{out}$ ) of the turbine rotor and the wind kinetic energy per unit time ( $P_{in}$ ) with the rotor swept area ( $A$ ), given as follows:

$$C_p = \frac{P_{out}}{P_{in}} = \frac{Q \cdot \omega}{0.5 \rho V_0^3 A} \quad (1)$$

Where  $A$  is the swept area of the rotor with the largest diameter,  $\rho$  is the air density, and  $V_0$  is the inlet wind speed of the turbine. The power coefficient is a nonlinear function of the blade tip speed ratio ( $\lambda$ ) or tip speed ratio (TSR), where TSR depends on the wind speed and the rotational speed of the shaft where  $R$  is the radius of the rotor. The TSR for the first rotor is calculated based on the following equation:

$$\lambda_1 = \frac{U_{tip,1}}{V_0} = \frac{R_1 \omega_1}{V_0} \quad (2)$$

The TSR for the second rotor is calculated based on the measurement results through the following equation:

$$\lambda_2 = \frac{U_{tip,2}}{V_0} = \frac{R_2 \omega_2}{V_0} \quad (3)$$

Where  $\omega_1$  and  $\omega_2$  are the angular velocity of the first and second rotor shafts, respectively.

### III. RESULTS AND DISCUSSION

#### A. Test result

The test is carried out based on the characteristics of the turbine with three variations of the rotor distance, namely:  $Z/D=0.4, 0.5,$  and  $0.6$ , where  $D$  is the front diameter, and for any change in wind speed. In Fig. 6 and Fig. 7, the measurement results of voltage and current are taken as an example of a test at a wind speed of  $8.64 \text{ m/s}$  and as a load of  $8 \text{ mm}$  blue LED lights with shaft rotation on the front rotor of  $3063 \text{ rpm}$  and the rear rotor of  $2566 \text{ rpm}$ . One test for any variation was taken 200 samples and then the average was taken.

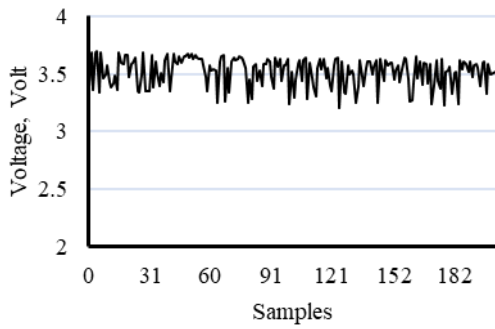


Fig. 6. Results of measurement of voltage.

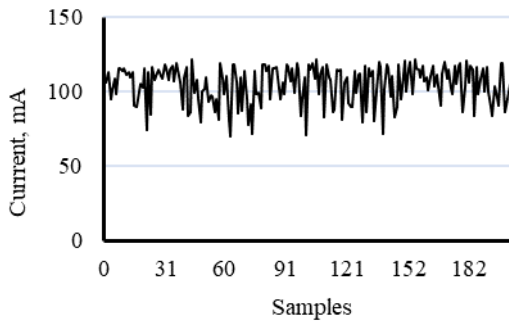


Fig. 7. Results of measurement of current.

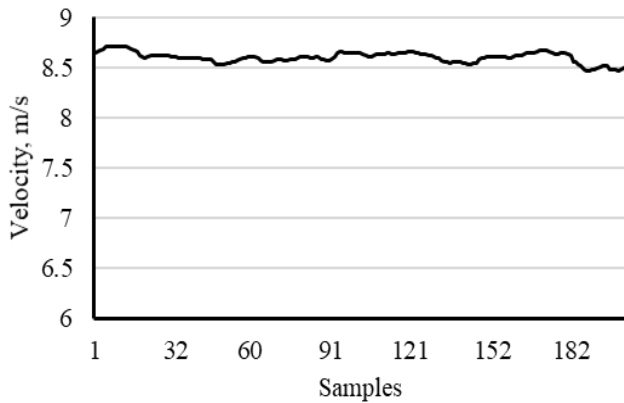


Fig. 8. Results of measurement of wind velocity

Fig. 8 shows the results of measuring wind speed with Hot Wire, where the recorded data is stored on a laptop in the form of a notepad. The loading on the turbine is carried out by varying the load of the LED lamps. The graph above contains 199 samples per point, these points are taken according to the time of testing for one load variation or wind speed, the period in testing for a variety of loads or wind speed ranges from 3-4 minutes

Test results as shown in Fig. 11 CRWT wind turbine output power relationship to wind speed variation from 3.07 m/s to 8.61 m/s. This graph shows that the power generated against the wind speed continues to increase, with the axial distance of the rotor  $Z/D=0.5$ , as a trend the polynomial line is higher than  $Z/D=0.4$  or  $Z/D=0.6$ . While the increase in turbine rotor rotation as shown in Fig. 12 forms the peak of the parabolic curve at the highest maximum output power at  $Z/D=0.5$  for both the front and rear rotors. This graph shows

the output power of the front rotor and rear rotor continues to increase with increasing rotation at  $Z/D=0.5$ , then decreases after the front rotor power coefficient reaches a peak closer to the single rotor.

The relationship between the turbine power coefficient from Equation 1 to the tip speed ratio from Equations 2 and Equations 3 as shown in Fig. 13 and Fig. 14 also shows the same thing, namely that the best performance of the CRWT turbine occurs at the distance ratio  $Z/D = 0.5$ . Fig. 13 shows the front rotor power coefficient at low TSR tends to be higher than the single rotor for all distance variations. As the TSR increases, once the power coefficient reaches its peak it decreases for all rotors. However, the front rotor at  $Z/D=0.5$  continues to experience an increase in the power coefficient with an increase in TSR which is almost the same as the single rotor. A different phenomenon occurs in the rear rotor, where at low and high TSR the rotor distance  $Z/D=0.6$  has the lowest power coefficient. Meanwhile, the rotor distance  $Z/D=0.5$  tends to have a better power coefficient than other distance variations at higher TSR. The two phenomena above as in Fig. 14 show that the best-combined power coefficient of the front rotor and rear rotor (CRWT) is at the rotor distance  $Z/D=0.5$  with a wider TSR.

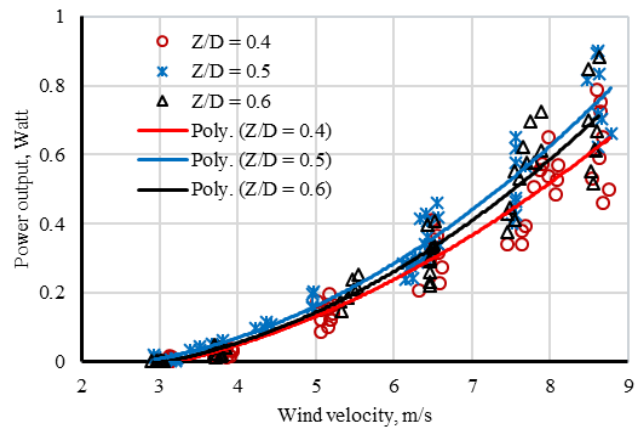


Fig. 9. The relationship of the CRWT wind turbine output power to the ratio of the rotor distance,  $Z/D=0.4, 0.5, \text{ and } 0.6$ , to variations in wind speed of 3.07 m/s to 8.61 m/s

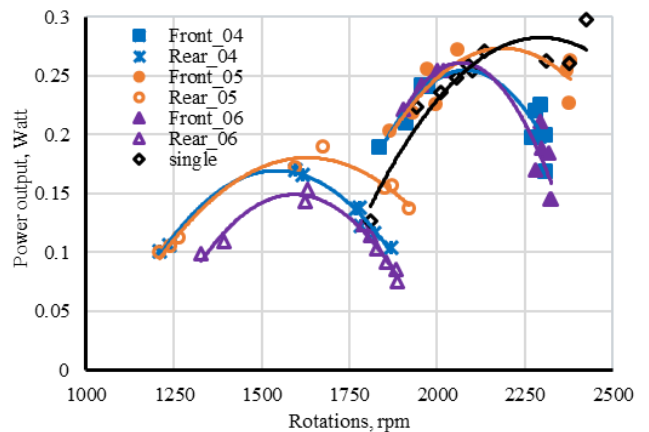


Fig. 10. Relationship of output power and front rotor rotation, rear rotor CRWT wind turbine for distance ratio  $Z/D=0.4, 0.5, \text{ and } 0.6$ , and single rotor wind turbine at average wind speed-average 6.51 m/s.

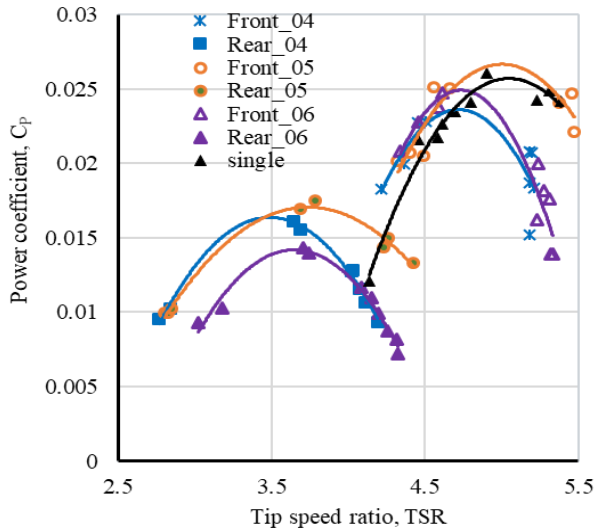


Fig. 11. The relationship between power coefficient and tip speed ratio of the front rotor, rear rotor wind turbine for the distance ratio  $Z/D=0.4, 0.5,$  and  $0.6,$  and single rotor wind turbines.

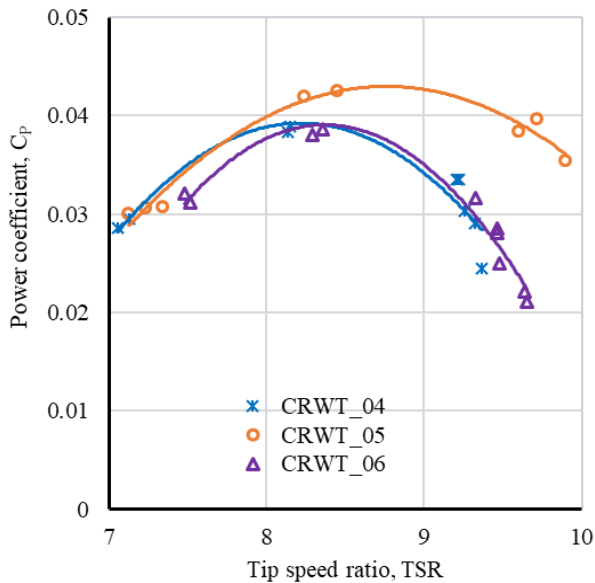


Fig. 12. The relationship between power coefficient and tip speed ratio of the CRWT wind turbine for the distance ratio  $Z/D=0.4, 0.5,$  and  $0.6.$

From Fig. 11 and Fig. 12 through the value of the peak power coefficient of the turbine is plotted against the variation of the rotor distance at three different wind speed conditions. At a wind speed of  $3.73 \text{ m/s}$ , it can be seen that the peak power coefficient occurs at a distance of  $Z/D=0.5$  both the front rotor, the rear rotor, and the combination of both (CRWT), see Fig. 13. The same trend also occurs at wind speeds of  $6.51 \text{ m/s}$  and  $8.61 \text{ m/s}$  as in Fig. 14 and Fig. 15. Maximum total power coefficients for each distance ratio of  $Z/D=0.4, 0.5,$  and  $0.6$  at wind speeds of  $6.51 \text{ m/s}$  are  $0.0389, 0.0425,$  and  $0.0387$  respectively. The relationship between the variation of the rotor distance to the total power coefficient of the front rotor and the rear rotor, it was found that the maximum power coefficient occurred at a distance of  $Z/D=0.5$

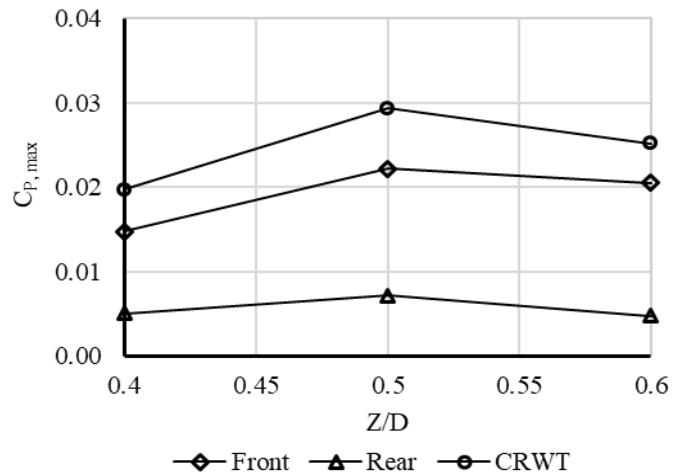


Fig. 13. The maximum power coefficient of the CRWT wind turbine at an average wind speed of  $3.73 \text{ m/s}$  with a variation of the ratio of the rotor distance  $Z/D=0.4, 0.5,$  and  $0.6.$

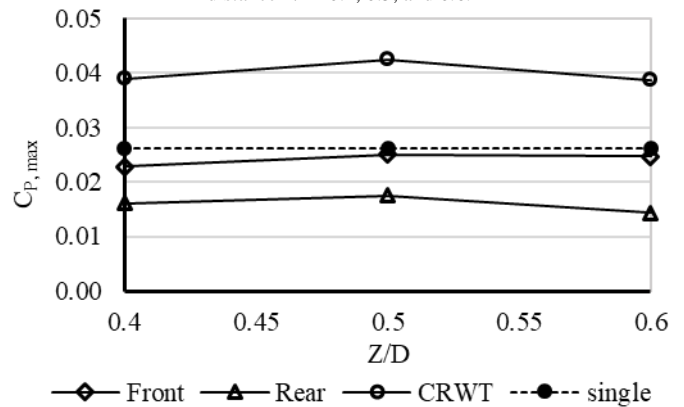


Figure 14. The maximum power coefficient of the CRWT wind turbine at an average wind speed of  $6.51 \text{ m/s}$  with a variation of the ratio of the rotor distance  $Z/D=0.4, 0.5,$  and  $0.6.$

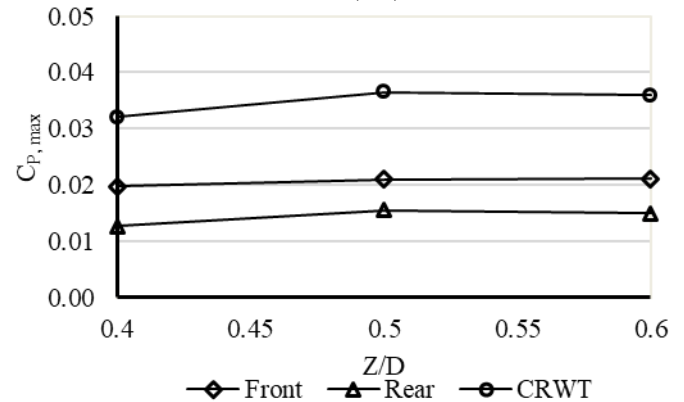


Figure 15. The maximum power coefficient of the CRWT wind turbine at an average wind speed of  $8.61 \text{ m/s}$  with a variation of the ratio of the rotor distance  $Z/D=0.4, 0.5,$  and  $0.6.$

#### IV. CONCLUSION

The performance of a counter-rotating wind turbine was studied successfully by the experimental method, where the turbine model is made on a laboratory scale. The front rotor power coefficient at low TSR tends to be higher than that of a single rotor for all distance variations. With the increase in

TSR, the front rotor at a distance of  $Z/D=0.5$  continues to experience an increase in the coefficient of power along with an increase in TSR which is also almost the same as a single rotor. While at low and high TSR, for the variation of the rotor distance  $Z/D=0.6$  has the lowest power coefficient. While the rotor distance  $Z/D=0.5$  tends to have a better power coefficient than other distance variations at higher TSR. The combined power coefficient between the front and rear rotors (CRWT) to the ratio of the rotor spacing, with the highest value of total power coefficient occurring at  $Z/D=0.5$  with a wider TSR range.

The relationship between the variation of the rotor distance to the peak power coefficient of the front rotor and the rear rotor, it was found that the peak power coefficient occurred at a distance of  $Z/D=0.5$ . Maximum total power coefficients for each distance ratio of  $Z/D=0.4, 0.5,$  and  $0.6$  at wind speeds of  $6.51$  m/s are  $0.0389, 0.0425,$  and  $0.0387$  respectively.

#### REFERENCES

- [1] R. W. Y. Habash, V. Groza, Y. Yang, C. Blouin, and P. Guillemette, "Performance of a contrarotating small wind energy converter," *ISRN Mech. Eng.*, vol. 2011, 2011.
- [2] J. C. Dai, Y. P. Hu, D. S. Liu, and X. Long, "Aerodynamic loads calculation and analysis for large scale wind turbine based on combining BEM modified theory with dynamic stall model," *Renew. Energy*, vol. 36, no. 3, pp. 1095–1104, 2011, doi: 10.1016/j.renene.2010.08.024.
- [3] S. Rehman, M. Alam, L. Alhems, and M. Rafique, "Horizontal Axis Wind Turbine Blade Design Methodologies for Efficiency Enhancement—A Review," *Energies*, vol. 11, no. 3, p. 506, 2018, doi: 10.3390/en11030506.
- [4] F. Massouh and I. Dobrev, "Investigation of wind turbine flow and wake," *J. Fluid Sci. Technol.*, vol. 9, no. 3, pp. JFST0025–JFST0025, 2014.
- [5] V. A. Koehuan, Sugiyono, and S. Kamal, "Investigation of Counter-Rotating Wind Turbine Performance using Computational Fluid Dynamics Simulation," in *IOP Conference Series: Materials Science and Engineering*, 2017, vol. 267, no. 1, p. 12034.
- [6] V. A. Koehuan, Sugiyono, and S. Kamal, "Numerical Analysis on Aerodynamic Performance of Counter-rotating Wind Turbine through Rear Rotor Configuration," *Math. Model. Methods Appl. Sci.*, vol. 13, p. 240, 2019.
- [7] W. Yuan, A. Ozbay, W. Tian, and H. Hu, "An experimental investigation on the effects of turbine rotation directions on the wake interference of wind turbines," *51st AIAA Aerosp. Sci. Meet. Incl. New Horizons Forum Aerosp. Expo. 2013*, no. January, pp. 1–16, 2013.
- [8] W. Yuan, W. Tian, A. Ozbay, and H. Hu, "An experimental study on the effects of relative rotation direction on the wake interferences among tandem wind turbines," *Sci. China Physics, Mech. Astron.*, vol. 57, no. 5, pp. 935–949, 2014, doi: 10.1007/s11433-014-5429-x.
- [9] A. Ozbay, W. Tian, and H. Hu, "A Comparative Study of the Wake Characteristics behind a Single-Rotor Wind Turbine and Dual-Rotor Wind Turbines," in *32nd AIAA Applied Aerodynamics Conference*, 2014, p. 2282.
- [10] A. Ozbay, W. Tian, and H. Hu, "An experimental investigation on the aeromechanics and near wake characteristics of dual-rotor wind turbines (drwts)," in *32nd ASME Wind Energy Symposium*, 2014, p. 1085.
- [11] Z. Wang, T. Wei, and H. Hu, "An Experimental Study on the Wake Characteristics of Dual-Rotor Wind Turbines by Using a Stereoscopic PIV Technique," in *34th AIAA Applied Aerodynamics Conference*, 2016, p. 3128.
- [12] A. Ozbay, W. Tian, and H. Hu, "Experimental investigation on the wake characteristics and aeromechanics of dual-rotor wind turbines," *J. Eng. Gas Turbines Power*, vol. 138, no. 4, p. 42602, 2016.
- [13] P.-Å. Krogstad, L. Sætran, and M. S. Adaramola, "Blind Test 3' calculations of the performance and wake development behind two in-line and offset model wind turbines," *J. Fluids Struct.*, vol. 52, pp. 65–80, 2015.
- [14] J. Bartl and L. Sætran, "Blind test comparison of the performance and wake flow between two in-line wind turbines exposed to different turbulent inflow conditions," *Wind Energy Sci.*, vol. 2, no. 1, pp. 55–76, 2017.